J. Synchrotron Rad. (1998). **5**, 1058–1060

Experimental apparatus for the study of photoabsorption processes of multiply charged ions by synchrotron radiation

M. Oura,[a]* T. M. Kojima,[b] Y. Awaya,[b]† Y. Itoh,[c] K. Kawatsura,[d] M. Kimura,[e] T. Koizumi,[f] T. Sekioka,[g] H. Yamaoka[a] and M. Cox[h]

[a]JAERI-RIKEN SPring-8 Project Team, Kamigori, Ako-gun, Hyogo 678-12, Japan, [b]The Institute of Physical and Chemical Research (RIKEN), Wako, Saitama 351-01, Japan, [c]Physics Laboratory, Josai University, Sakado, Saitama 350-02, Japan, [d]Kyoto Institute of Technology, Matsugasaki, Sakyo-ku, Kyoto 606, Japan, [e]Kochi University of Technology, Tosayamada, Kochi 782, Japan, [f]Department of Physics, Rikkyo University, Toshima-ku, Tokyo 171, Japan, [g]Faculty of Engineering, Himeji Institute of Technology, Himeji, Hyogo 671-22, Japan, and [h]Accelerator Technology Group, Oxford Instruments, Oxford OX2 0DX, UK. E-mail: oura@sp8sun.spring8.or.jp

(*Received 4 August 1997; accepted 3 November 1997*)

Photon–ion merged-beam apparatus using a compact ECR ion source and a high-brilliance light source has been designed for the study of photoabsorption processes of multiply charged ions. Photoion spectroscopy will be performed along isoelectronic, isonuclear and isoionic sequences. The main features of this apparatus are described.

Keywords: spectroscopy; photoabsorption; multiply charged ions; electron cyclotron resonance ion source (ECRIS).

1. Introduction

Photoabsorption of ions (including multiply charged ions, MCI) is an important process for the understanding of astrophysical problems and plasma physics, especially in controlled thermonuclear fusion applications. Although the basic information on ions, such as photoabsorption cross section, binding energies of each shell, ionization potential *etc.*, are needed for a better understanding of such problems, experimental studies on the photoabsorption of ions are scarce because of the difficulties in achieving a high enough density of target ions. Most experimental studies of the interaction between photons and positive ions have been made by absorption spectroscopy by means of two laser-produced plasmas and by photoion spectroscopy for some singly charged ions at low photon energies using photon–ion merged-beam techniques (for a review, see Wuilleumier *et al.*, 1994, and references therein).

In the past decade we have developed a prototype apparatus using the photon–ion merged-beam method (Oura *et al.*, 1994; Koizumi *et al.*, 1995) and have measured a variety of photoion-yield spectra of singly charged ions and also some doubly or triply charged ions in the vacuum ultraviolet region (Itoh *et al.*, 1995; Sano *et al.*, 1996; Koizumi *et al.*, 1996, 1997). From these experiences, we designed a new photon–ion merged-beam apparatus to study the characteristics of MCI of further species and in a wider energy region by using high-brilliance synchrotron radiation. This apparatus enables us to perform systematic studies along isoelectronic, isonuclear and isoionic sequences in a wide range of electronic and charge states. It will supply more information on the changes in the characteristics and the dynamics of MCI as the nuclear charge or ionicity is changed.

The main components of the apparatus are an ion source, an ion beam transport system, an interaction region and an analyser for product ions. A schematic view of the apparatus is shown in Fig. 1. In the following section we describe briefly the outline of the overall assembly. The layout of the new apparatus and its pumping system are described in §3.

2. Outline of the overall assembly

2.1. *Ion source and ion beam transport system*

A compact electron cyclotron resonance ion source (ECRIS), NANOGAN (Sortais *et al.*, 1995), composed of FeNdB permanent magnets, is employed as the MCI source. The source body, placed at a positive potential (normally at 10 kV extraction voltage), consists of a plasma chamber, permanent magnets, a single-electrode extraction (adjustable and insulated for current measurement), a ceramic insulator for extraction exit (diameter 165 mm with elastomer seal), a UHF coupling system, a coaxial copper tube for gas injection in the plasma chamber, and an insulated mechanical support of the source (Fig. 2). This coaxial tube and the extraction diaphragm can be adjusted to the optimum position inside the plasma chamber. The flow rate of gas from the plasma chamber is 2–4 Pa m^3 s^{-1} in the extraction region when the source is in a typical operation condition. The source is pumped *via* the turbomolecular pump fitted to the first slit vessel.

Ions produced in the plasma chamber are accelerated by the extraction voltage of 10 kV. These ions are focused onto the entrance slits of the charge-selecting magnet by the first Einzel lens. Two sets of deflectors are located between the first Einzel lens and the entrance slits. Each set of deflectors consists of four electrostatic plates to steer the beam both in angle and displacement in the horizontal and vertical directions. These deflectors

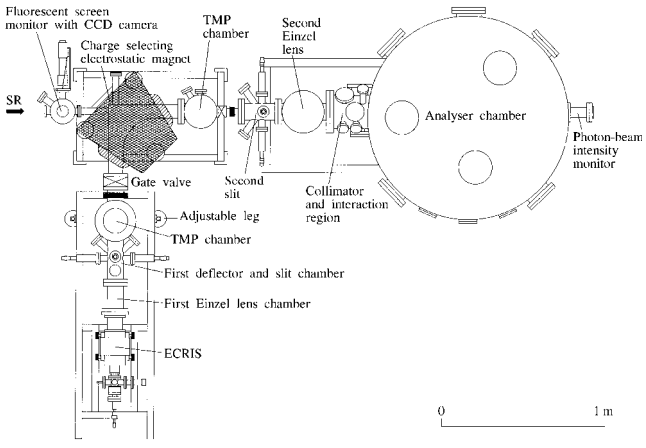

Figure 1
Schematic diagram of the photon–ion merged-beam apparatus (SR = synchrotron radiation).

† Present address: Musashino Art University, Kodaira, Tokyo 187, Japan.

also have a TTL (transistor–transistor logic) controlled beam blanking function. In the beam blanked mode, the beam hits the aperture plate in front of the entrance slits.

The specific ions in the primary beam are selected by the charge-selecting magnet. This magnet is a double-focus 90°-sector magnet with an orbital radius of 270 mm. The maximum field is in excess of 0.4 T, which allows it to cover a mass-to-charge ratio up to 70. The uniformity of the field is within 0.1% in the volume within ±20 mm around the beam axis. This magnet works also as a momentum selector and a beam merger.

The mass-selected ion beam is now merged into the photon beam and is focused onto the second slits which are located at the image point of the selector magnet. The diverging ion beam is again focused onto the collimator, consisting of a pair of 2 mm-diameter orifices (100 mm apart), by the second Einzel lens. This collimator defines the ion beam size and divergence before it enters the interaction region, the length of which is 120 mm.

2.2. *Interaction region*

In the interaction region the ion beam and the monochromatic photon beam will be collinearly merged so as to interact with each other. The interaction region is biased at a certain voltage (normally at 8 kV) in order to distinguish the product ions of a higher charge state from background ions produced outside this region.

The interaction region is equipped with a couple of beam-scanning devices to measure the beam profile at three points along the beam axis. One is for the vertical and the other is for the horizontal profile. Each set of devices comprises three slit holders and are mounted on a linear actuator. These devices enable the degree of overlapping of the beam density to be measured (form factor), which is required to determine the absolute photoabsorption cross sections. The interaction region is also equipped with an electron gun and a Faraday cup for calibration of the charge state analyser for product ions.

2.3. *Charge state analyser for product ions*

When an inner-shell electron of a target A^{q+} ion, where A is the atomic symbol and q is the charge state, is excited by photons, it emits electrons through Auger (or very often multiple Auger) processes and $A^{(q+1)+}$, $A^{(q+2)+}$, . . . , $A^{(q+n)+}$ ions are produced. On exiting the interaction region, these ions are re-accelerated by the voltage applied there. They have different kinetic energies according to their charge state ($q + i$). The resulting mixed-ion beam then strikes a cylindrical-mirror-type electrostatic charge state analyser (Sar-el, 1967), the geometry of which is chosen to produce first- and second-order focusing of the primary beam, so as to be separated into its constituents. Different ionic species are deflected by the radial electrostatic field of the analyser to differing extents according to their kinetic energies and charge states.

The radii of the inner and outer cylinder of the analyser are 82 and 180 mm, respectively, and the overall length is 700 mm. The entrance angle is 42.3° to the cylinder axis. The exact design of the analyser and location of the pulse-counting position-sensitive detector (PSD) have been determined by computer simulation. The inner cylinder is normally at ground potential and the outer cylinder will be biased at 6 or 5.5 kV to cover the wide range of charge states of the product ions. Two identical Faraday cups are arranged to intercept the primary beam at different positions corresponding to these different operating voltages of the analyser. The resulting charge distribution of the product ions will be analysed according to their spatial distribution on the PSD. Calibration of the PSD will be performed by measuring the intensity ratios of the product ions which are ionized by electron impact and by comparing those results with existing absolute measurements.

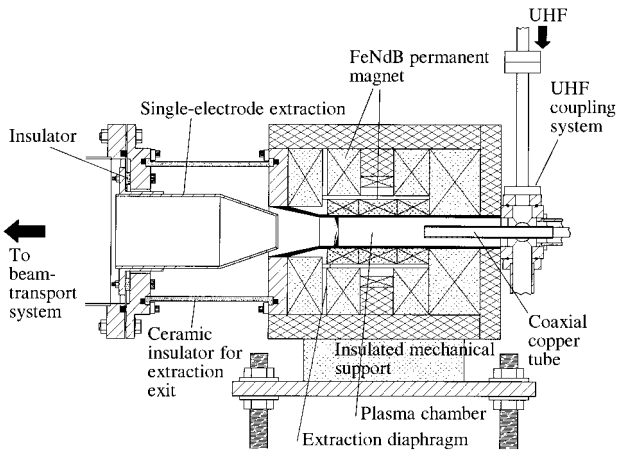

Figure 2
Schematic view of the ion source.

3. Layout and vacuum system

3.1. *Layout of the apparatus*

The dimensions of the apparatus are about 3.6 × 2.8 m. The support frame is mounted on a number of adjustable legs allowing for ±10 mm continuous adjustment in X and Y (horizontal) and ±20 mm continuous adjustment in Z (vertical). These adjustable legs enable the height range to be 1260 ± 20 mm. By combining with the optional spacer plates, the apparatus will cover the entire height range from 1240 to 1490 mm.

Beside the apparatus there are a UHF power generator for the ion source and several standard racks to operate the apparatus. A 200 W 10 GHz microwave power generator is located beside the ion source and the power will be transferred through the wave guides.

3.2. *Vacuum system*

The vacuum system can be divided into four sections, *i.e.* the ducts and vessels from the ion source to the first slits, the selector magnet vessel, the vessels from the second slits to the collimator, and the analyser vessel. Each section has its own pumping system and can be isolated by UHV gate valves. The first section (from the ion source to the first slits) is pumped by a 1600 l s^{-1} turbomolecular pump backed with an oil-free diaphragm pump, and the pressure before the selector magnet will be maintained to be better than 6×10^{-5} Pa during ion source operation. A 500 l s^{-1} turbomolecular pump backed in common with the backing pump of the upstream section is used to evacuate the selector magnet section. The pumping system for the third section (from the second slits to the collimator) is identical to that of the first section. A pressure of 1.3×10^{-7} Pa will be maintained during the measurement. As for the final section, *i.e.* the analyser vessel, it is pumped by an argon stable ion pump (480 l s^{-1} pumping speed) and a titanium sublimation pump of surface area

approximately 2500 cm^2. These pumps maintain a UHV condition of better than 6×10^{-9} Pa in the analyser vessel when the beam passes through both the interaction region and the analyser, in order to increase the signal-to-noise ratio since the main part of the noise comes from charge-exchange processes of the primary ions with the residual gas. The vacuum pressure of these four sections is monitored by ionization vacuum gauges which are controlled by a multi-gauge power supply.

References

Itoh, Y., Koizumi, T., Awaya, Y., Kravis, S. D., Oura, M., Sano, M., Sekioka, T. & Koike, F. (1995). *J. Phys. B*, **28**, 4733–4742.

Koizumi, T., Awaya, Y., Fujino, A., Itoh, Y., Kitajima, M., Kojima, T. M., Oura, M., Okuma, R., Sano, M., Sekioka, T., Watanabe, N. & Koike, F. (1997). *Phys. Scr.* T**73**, 131–132.

Koizumi, T., Awaya, Y., Gonno, M., Itoh, Y., Kimura, M., Kojima, T. M., Kravis, S., Oura, M., Sano, M., Sekioka, T., Watanabe, N., Yamaoka, H. & Koike, F. (1996). *J. Electron Spectrosc. Relat. Phenom.* **79**, 289–292.

Koizumi, T., Itoh, Y., Sano, M., Kimura, M., Kojima, T. M., Kravis, S., Matsumoto, A., Oura, M., Sekioka, T. & Awaya, Y. (1995). *J. Phys. B*, **28**, 609–616.

Oura, M., Kravis, S., Koizumi, T., Itoh, Y., Kojima, T. M., Sano, M., Sekioka, T., Kimura, M., Okuno, K. & Awaya, Y. (1994). *Nucl. Instrum. Methods*, B**86**, 190–193.

Sano, M., Itoh, Y., Koizumi, T., Kojima, T. M., Kravis, S. D., Oura, M., Sekioka, T., Watanabe, N., Awaya, Y. & Koike, F. (1996). *J. Phys. B*, **29**, 5305–5313.

Sar-el, H. Z. (1967). *Rev. Sci. Instrum.* **38**, 1210.

Sortais, P., Bieth, C., Foury, P., Lecesne, N., Leroy, R., Mandin, J., Marry, C., Pacquet, J. Y., Robert, E. & Villari, A. C. C. (1995). *Proceedings of the 12th International Workshop on ECR Ion Sources*, edited by M. Sekiguchi & T. Nakagawa, pp. 44–52. Tokyo: Institute for Nuclear Study.

Wuilleumier, F. J., Bizau, J. M., Cubaynes, D., Rouvellou, B. & Journel, L. (1994). *Nucl. Instrum. Methods*, B**87**, 190–197.